Available online at www.sciencedirect.com
ScienceDirect
ELSEVIER
Sensors and Actuators A 134 (2007) 20–26
SENSORS AND ACTUATORS A PHYSICAL
www.elsevier.com/locate/sna

A single cell electrophysiological analysis device with embedded electrode

Sha Li *, Liwei Lin

Berkeley Sensor and Actuator Center, Department of Mechanical Engineering, University of California at Berkeley, 1113 Etcheverry Hall, UC Berkeley, Berkeley, CA 94720-1740, USA

Received 28 February 2006; accepted 11 April 2006
Available online 16 June 2006

Abstract

A single cell electrophysiological analysis device with a sub-micrometer opening on embedded recording electrode has been demonstrated using a combined micro- and nano-machining process. This technique can reduce the series pipette resistance while keeping high seal resistance for electrophysiological measurements. In the prototype demonstration, the electrolyte pipette resistance is reduced to 200 kΩ using the microfabricated electrophysiological system with opening size of 500 nm in diameter. A 6 GΩ seal resistance is achieved on a HeLa cell, a cervical cancer cell line with size between 10 and 20 μm, on the same device. In a second experiment, the measured electrolyte pipette resistance is 1 MΩ using different pipette solution on a device with 800 nm opening and a 500 MΩ seal resistance is achieved on a vacuolar yeast cell of 3–5 μm in size.
© 2006 Published by Elsevier B.V.

Keywords: Electrophysiological analysis; Patch clamp; Electrolyte pipette resistance; Seal resistance

1. Introduction

Patch clamp is one of the most important and powerful tools for ion channel related studies for electrophysiological measurements, and has been widely used in bio-related research and medicine development since it was first introduced by Neher and Sakmann in 1976 [1]. The basic function of the patch clamp, which is inherited from the old voltage clamp technique, is to detect the ion channel current flowing in/out the cell through proteins embedded in the lipid membrane using a glass pipette. The activities of various ion channels under different physical and chemical stimulations and the communications between cells have been studied with the assistance of patch clamps and these studies greatly expand our understanding of fundamentals of cells and the whole biological systems [2].

After more than 20 years of refinement, patch clamp has become mature and standard technique for ion channel measurement. However, the patch clamp experiment itself is very laborious, time consuming and requires a lot of experience to get satisfying results, therefore planar patch clamps have been proposed to reduce the experimental complexity with batch manufacturing processes as a high-throughput tool for potential drug discovery applications [3–14]. Whatever schemes you use, the basic one or the recently proposed planar ones, there are still issues associated with the patch clamp working principles. For example, firstly, the resistance of the pipette from the solution is always part of the whole recording circuit and this series resistance can distort the voltage measurements and the injected current. This resistance is also normally non-linear and sometimes unstable such that it is difficult to fully compensate [15]. Therefore, the first research goal of this work is the reduction of this serial resistance. Secondly, the relatively big openings of common patch clamps (μm range) and the correlated series resistance issue add more difficulty in recording small cells such as yeast and *E. coli*. Therefore, the second research goal of this work is to make sub-micrometer opening holes in building up the measuring system. In contrast to the traditional patch clamps using electrolyte as part of the electrode, this paper presents the approach of constructing an in situ electrode which is close to the patch to reduce the series (built-in) resistance. FIB (focus ion beam) technique is used to fabricate the opening holes in the sub-micrometer range for electrophysiological studies of cells less than 5 μm in diameter [16]. This paper will further elaborate

* Corresponding author. Tel.: +1 510 642 8983; fax: +1 510 643 6637.
E-mail addresses: shali@me.berkeley.edu, shali@newon.berkeley.edu (S. Li).

0924-4247/$ – see front matter © 2006 Published by Elsevier B.V.
doi:10.1016/j.sna.2006.04.034

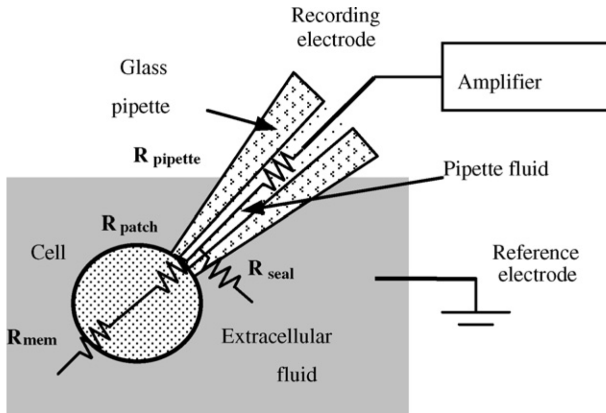

Fig. 1. The concept of the conventional patch clamp [2].

the circuit model in both conventional and our setup as well as issues in series resistance.

2. Theoretical analysis

Fig. 1 illustrates the conventional patch clamp experiment by a glass pipette that is fabricated by heating and pulling a glass or quartz tube to form a sharp tip with end diameter in the range of 1–20 μm. Before the experiment, the pipette is filled with conductive electrolyte to serve as the recording "electrode" and the electrode pipette resistance is determined by the tip size and geometry of the pipette with a typical range of 5–10 MΩ if the tip is 1 μm in diameter and 10–90 MΩ if the tip is submicron [17]. The cell solution is placed under a microscope while the pipette approaches a single cell under the control of a micromanipulator. When the pipette touches the surface of the cell, suction is applied from the backside of the pipette by a syringe or mouth to form a local seal, leading to a high resistance between the recording electrode and the reference electrode that is placed in the solution as illustrated. This step is critical for the patch clamp experiments because the ion channel signal is very small and a high seal resistance can reduce the leakage current and improve the signal-to-noise ratio.

An analytical model of patch clamp can be easily established from Fig. 1. $R_{pipette}$ is the resistance of electrolyte between the recording electrode and the cell. R_{patch} is the resistance of cell membrane portion inside the hole and R_{mem} is the membrane resistance outside the hole. R_{seal} is the resistance due to the leakage between the cell and the device, which is normally called seal resistance. If a potential difference, V_a, is applied between the two electrodes, the voltage applied on the cell is

$$V_c = \frac{V_a}{R_{pipette} + R_{seal}//(R_{patch} + R_{mem})} \times (R_{seal}//(R_{patch} + R_{mem})) \quad (1)$$

and the current flowing to the recording electrode is

$$I_d = \frac{V_a}{R_{pipette} + R_{seal}//(R_{patch} + R_{mem})} \quad (2)$$

In this system, the opening and closing of ion channels on the lipid membrane will affect R_{patch} and R_{mem} and it is easy to see that R_{patch} is much higher than R_{mem} because the tip size of the pipette is definitely smaller than the cell size. In order to get good signals from the measurement and make sure they can effectively reflect the real cell activities, we have to reduce the error between V_c and V_a and keep the value I_d as close to $V_a/(R_{patch} + R_{mem})$ as possible. Therefore a low electrolyte pipette resistance $R_{pipette}$ and a high seal resistance R_{seal} are highly desirable in the experiment.

There are two main configurations in patch clamp measurement, the cell-attached patch mode and the whole-cell mode. The cell-attached patch mode is normally used to study the individual ion channel activities so the potential between two electrodes is typically clamped at a fixed voltage and the current is recorded to represent the open and close status of ion channels. In this case, the ion channel signal is in the order of pA. The whole-cell mode is used to study the activities of all ion channels on a cell. The patch clamped membrane underneath the tip is ruptured by a stronger suction after the seal is achieved and a series of pulses with different potentials are added between two electrodes while the signal normally ranges from pA to nA. The voltage clamped between two electrodes is normally in tens of millivolt range to hundreds of millivolt in both configurations so the $R_{patch} + R_{mem}$ can range from tens of MΩ to GΩ under stimulations. Hence, according to Eq. (2), the seal resistance R_{seal} is better to be higher than GΩ, or so called "GΩ seal", which is in the same order of the patch resistance.

The electrolyte pipette resistance can be measured without clamping the cell on the device and the typical value is several MΩ for normal tip sizes. It can be neglected in Eq. (2) as compared with seal resistance and patch resistance. However, the state-of-art patch clamp techniques are limited to a trade-off between small pipette tip size and small pipette resistance. And for the single ion channel or small cell detection, a small tip size device (down to the sub-micron range) has to be used. As a result, the electrolyte pipette resistance from a conventional glass pipette can increase to 10–90 MΩ [17] and this could reduce the accuracy of the voltage clamp result, especially in the whole-cell recording configuration, where the cell is ruptured and $R_{patch} = 0$. In that case, the electrolyte pipette resistance could be in the same range of the membrane resistance, R_{mem} such that the recording results are greatly distorted. Currently, in order to solve this problem, researchers conduct biological modifications on small cells to enlarge the cell size and/or reduce the expressed ion channel densities on a single cell so that a normal tip size pipette can be used for the ease of the experiments [18,19].

3. Experiment

3.1. Device fabrication

The electrophysiological device is fabricated on a phosphorous doped, 4 in. in diameter, 525 μm thick <1 0 0> silicon wafer and the fabrication process is shown in Fig. 2. A positive G-line photoresist is used in the process except indicated and all the photolithography process is done by Karl Suss MA6 Mask Aligner. A 100 nm thick wet oxide is grown on both side of the

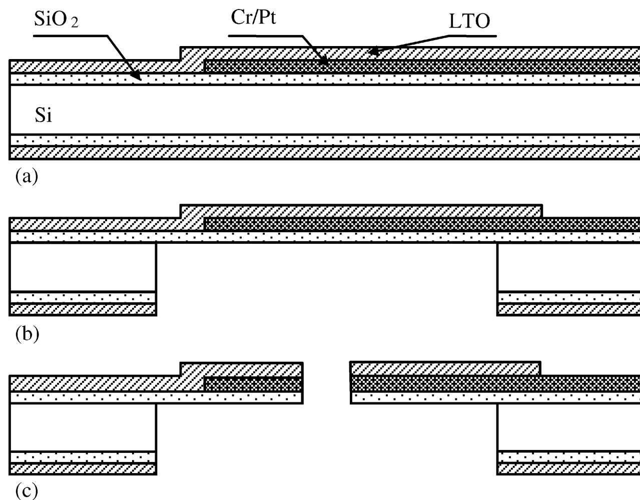

Fig. 2. The fabrication process of the MEMS patch clamp device.

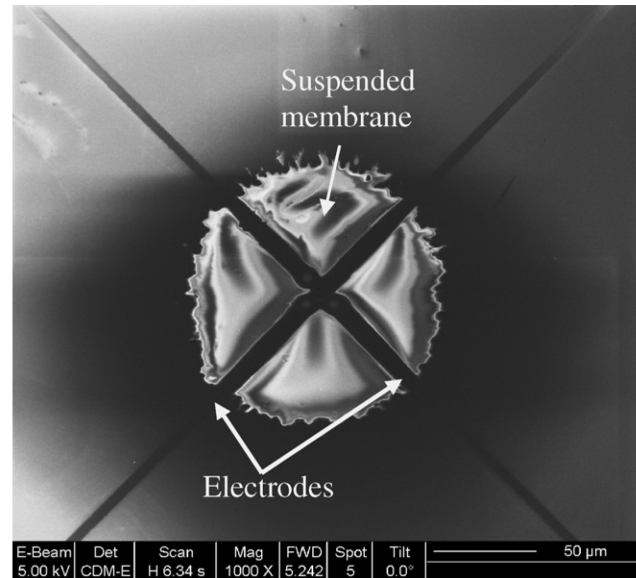

Fig. 3. SEM picture of a 100 μm in diameter membrane with four recording electrodes.

wafer at 900 °C in a furnace as an insulation layer. A 1.1 μm thick I-line positive resist is spun on the top side of the wafer and patterned by the first lithographic process. Then the wafer is hard-baked at 120 °C for 2 h. A Cr/Pt layer (10 nm/100 nm) is sputtered on the wafer by a Randex DC sputtering system and after the lift-off process using sonication in acetone, the electrodes are constructed. Afterwards the wafer is thoroughly cleaned in DI water and put back to a LPCVD furnace where a 200 nm thick LTO (low temperature oxide) is grown on top of the electrodes. This LTO layer will serve as an insulation layer in the later experiment. Fig. 2(a) applies after these steps. The second lithographic process defines the contact pad on the LTO layer with a RIE (reactive ion etching) silicon oxide etcher. Next step, a 2 μm thick photoresist is spun on the front side of the wafer and four layers of 2 μm thick G-line photoresist are spun on the back side of the wafer to serve as the etch mask for the through-wafer etching process. A backside alignment is used in the third lithographic process to define the backside holes. Then, a RIE oxide etch process is conducted to get rid of the oxide layer on the holes at the back side of the wafer and a DRIE (deep reactive ion etching) etching is preformed by a STS (Surface Technology Systems) multiplex ICP ASE system (Inductively Coupled Plasma Advanced Silicon Etcher) to etch silicon all the way through the wafer until reaching the oxide on the front side as shown in Fig. 2(b). The typical hole size is 100 μm in diameter. During this through-wafer etching process, separation lines are also defined and etched such that individual testing chips are separated (still in connection with a thin oxide layer) concurrently during the DRIE process.

After these fabrication steps, a suspended membrane with embedded electrodes protected by both top and bottom insulation layers of SiO_2 is created. The chip is then placed in a FIB system (a FEI Strata 235M dual beam (FIB/SEM) FIB system). Inside the FIB, the working electrode embedded in the SiO_2 membrane is located using SEM and a hole with size from 100 nm to 1.5 μm in diameter is drilled by ion beams through the sandwiched membrane by a 30 keV gallium ion column as shown in Fig. 2(c). The beam current used in FIB ranged from 50 to 300 pA to get various hole openings and the normal drilling time is about 30 s–1 min for each individual hole openings.

Fig. 3 shows the SEM microphoto of a 100 μm in diameter thin membrane with four potential recording electrodes. It can be observed that the perimeter of the backside hole is irregular and the reason for this phenomenon is the footing problem during the DRIE process [20], which is the result of ions that cannot escape from the deep trench during etching due to the structure's high-aspect-ratio nature. The footing problem can be minimized by using lower frequency etching power in the ICP system but this will decrease the etching rate. In our case, this irregular feature has minimum impact on the functionality of the device. From Fig. 3, we can also see the SiO_2 membrane is buckled. This is actually a temporary deformation caused by the tem-

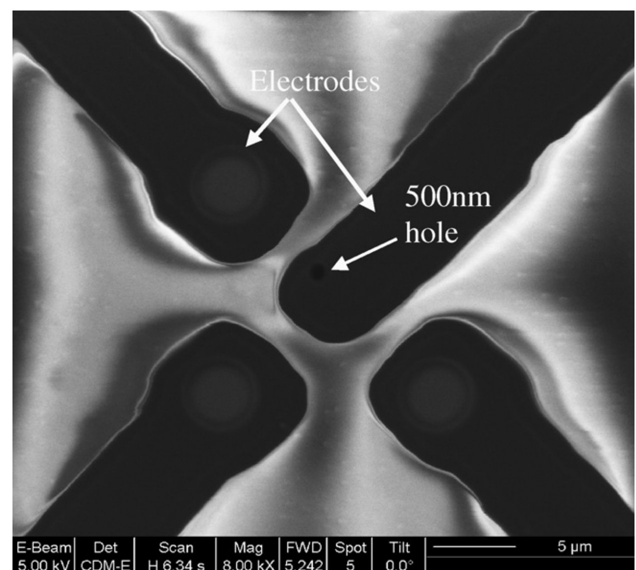

Fig. 4. Close-up view of the four electrodes in Fig. 3. A 500 nm in diameter hole was drilled on the upper-right electrode.

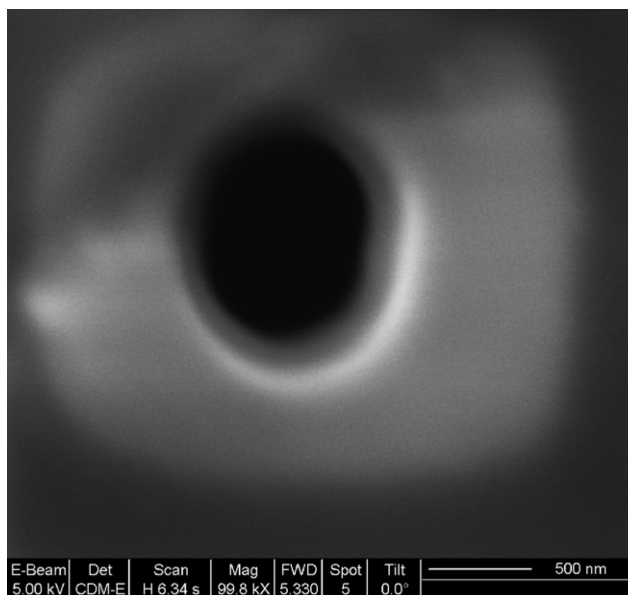

Fig. 5. The close-up of the 500 nm in diameter hole.

perature raise on the oxide membrane due to the bombardment of electrons. As electrons hit on the sample surface, the kinetic energy of moving particles converts into the thermal energy and is generally conducted away very quickly via underneath silicon heat sink. The membrane area is made of silicon dioxide with poor thermal conductivity that causes temperature rise and thermal deformation as shown. This deformation is observed to be bigger as the scanning times increase. Fig. 4 is the close-up view of the electrodes in Fig. 3 and a 500 nm in diameter hole was drilled on the upper-right electrode. The width of the electrodes is 4 μm. Fig. 5 shows the close-up of the 500 nm hole.

The experimental setup is illustrated in Fig. 6. A metal wire is soldered on the contact pad as shown. A 5 mm-high 0.125 in. inner diameter silicone tube is glued with superglue on the top surface of the chip to form a cell chamber. A 0.0625 in. inner diameter silicone tube is glued on the backside of the chip using a "5-minute epoxy" and connected to a syringe or a syringe pump in order to provide negative pressure from the hole. Fig. 6 also shows circuit representation of the on-chip path clamp device. It is observed when compared with Fig. 1 that the circuit representation of this device is very similar to the conventional patch clamp model while the in situ recording electrode could reduce the R_{pipette} resistance.

3.2. Cell culture

Two kinds of cells, HeLa cells and yeast cells (*Saccharomyces cerevisiae* strain BY4742), are used to investigate the pipette resistance and seal resistance on the micro-fabricated chips. HeLa cells (a human cervical cancer cell line) are cultured in DMEM:F12 media (50:50), supplemented with 10% fetal bovine serum, penicillin/streptomycin, and L-glutamine at 37 °C in a humidified 5% CO_2, 95% air atmosphere. Before the experiments, most culture media are suck and cleared out and the cells are treated by 200 μl trypsin (0.05% trypsin, 0.02% versene, in saline) to detach cells from the culture plate. Afterwards, 200 μl culture media are added to neutralize the effect of trypsin. Yeast cells are also tested for verification of possibilities of patch clamping small cells. A single colony of yeast cells are first incubated in 10 ml YPD (20 g/l bacteriological peptone, 10 g/l yeast extract, 20 g/l glucose) liquid media overnight at 30 °C. A 2 ml volume of the fresh cell culture is centrifuged at 6000 rpm for 5 min and the cell pellet is rinsed twice and re-suspended in 2 ml, 300 mM NaCl solution.

3.3. Experimental process

The setup of the experiment is shown in Fig. 7. The pipette solution is backfilled into the backside tube on the device, which is then connected to a syringe. For HeLa cell experiment, the pipette solution used is ND96 solution, which consists of 6 mM NaCl, 2 mM KCl, 1.8 mM $CaCl_2$, 1 mM $MgCl_2$, and 5 mM HEPES, and is regulated to pH 7.6. For yeast cell, the pipette solution is 300 mM NaCl solution. Then, the cell solution is filled into the top chamber. A Pt wire is inserted into the top chamber to serve as the reference electrode during recording. Both Pt wire and the in situ electrode are connected to a signal amplifier (HP 4156B semiconductor parameter analyzer). A 10 mV constant voltage was added on the recording electrode and the current was recorded before any cell was attached on the

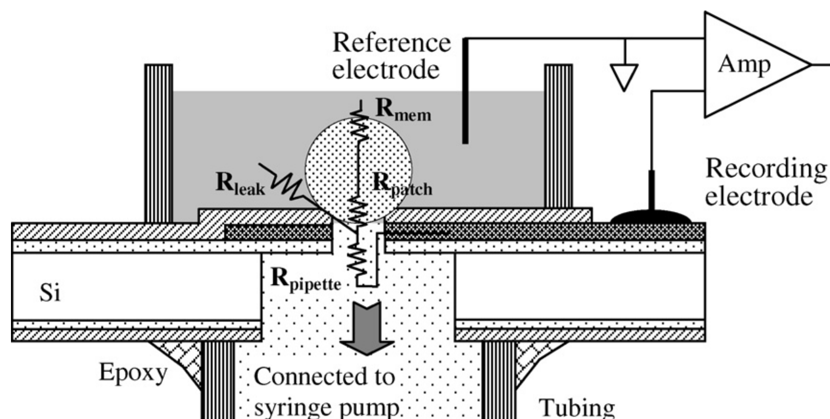

Fig. 6. Schematic setup of the single cell electrophysiological analysis via the sub-micrometer opening (not in scale).

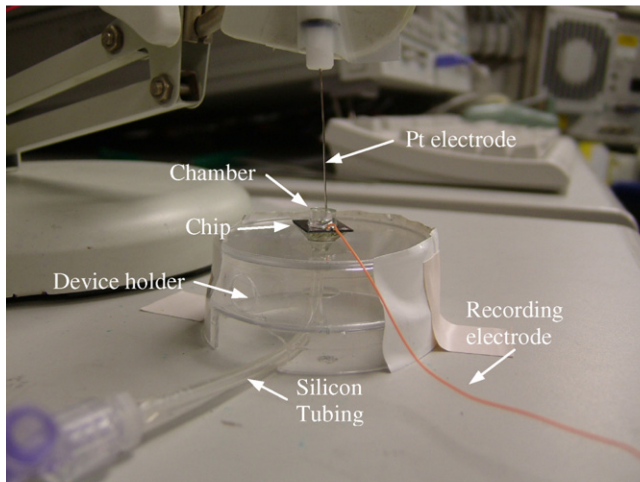

Fig. 7. The experimental setup.

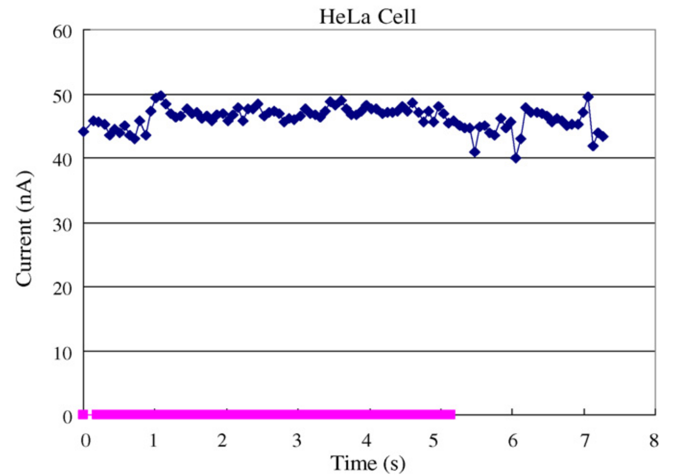

Fig. 9. Current responses of a HeLa cell before and after the seal formed on a device with a 500 nm opening.

hole to measure the electrolyte pipette resistance. Afterwards, a constant suction was applied through the backside tubing by the syringe and cells were observed to gradually move towards the hole until a single cell is positioned on top of the hole as shown in Fig. 8. The current between two electrodes is measured again to calculate the seal resistance of the device. When the current on the recording electrode drops several orders of magnitude, a good seal between the sub-micrometer hole and the cell is established.

3.4. Results and discussion

Using the methods described above, the tests are performed on both cells. Fig. 9 shows the recorded current before and after the seal is achieved for the HeLa cell on a device with a 500 nm opening. From the plot, the pipette resistance is estimated as 200 kΩ before the seal and the seal resistance is 6 GΩ. Fig. 10 shows the current measurement results before and after the seal is formed for the yeast cell on a device with an 800 nm opening. The pipette resistance is estimated as 1 MΩ and the seal resistance is 500 MΩ. This relatively low seal resistance is expected due to the vacuole of yeast and can be improved by dissolving the vacuole to expose the internal plasma membrane. From these results, we have demonstrated that the pipette resistance of the 500 nm opening is 200 kΩ and that is at least one order of magnitude reduction when compared with a normal patch clamp setup and the GΩ seal on the HeLa cell is achieved.

Although low electrolyte pipette resistance, R_{pipette}, and a high seal resistance, R_{seal}, have been achieved successfully in our experiments, the yield of the GΩ seal is still relatively low. The possible reasons are: (1) some openings are not in prefect circular shapes as constructed by the FIB process due to beam shifting phenomena; (2) the edge of the hole is not smooth sometime due to vibrations of the ion beam; (3) the surface around the hole is not flat due to the redeposition of the materials during the drilling process. These are all minor irregularities while the combination may affect the experiments greatly. Several approaches may alleviate these problems. For example, a shorter drilling time can reduce the probability of beam shifting and ion beam variations while a lower FIB current can eliminate the redeposition of materials [21].

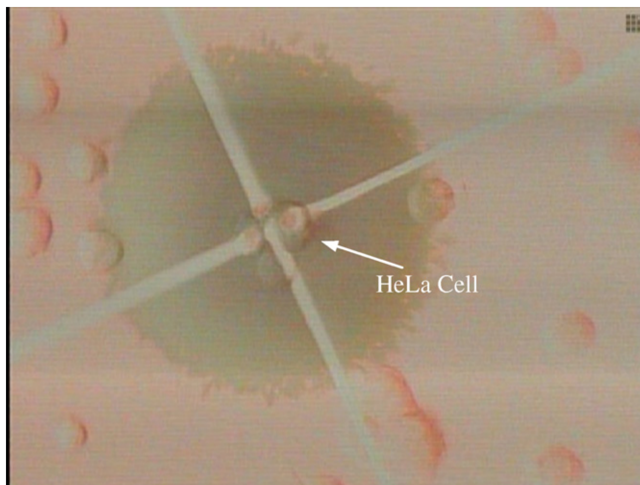

Fig. 8. Top view of the chip with 500 nm hole after trapping a HeLa Cell on the hole.

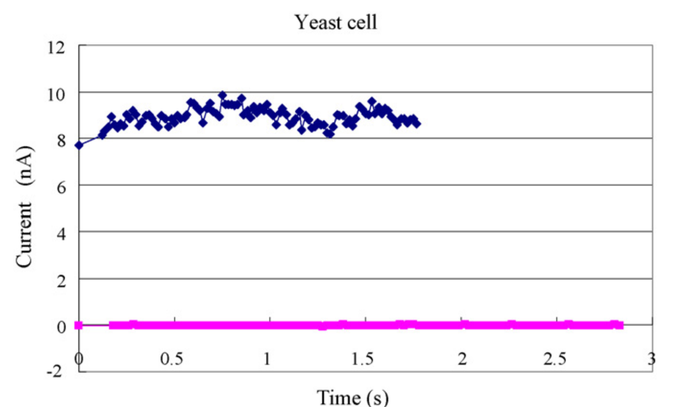

Fig. 10. Current responses of a yeast cell before and after the seal is formed on a device with an 800 nm opening.

Furthermore, gallium has very low melting point and is easy to generate the ion column so it has been the common material in FIB. However, it has also been reported [22] that gallium ions might contaminate the devices during the fabrication process. One critical problem is that injected gallium content can make the silicon dioxide insulation layer become somewhat conductive and add another current path between two electrodes to drastically affect the GΩ seal. This issue is further studied by using 500 and 1000 pA ion currents to drill 5 μm in diameter openings between two different pairs of electrodes. EDS is used to analyze the chemistry contents of the materials around the drilled openings. Both samples show the existence of gallium within an area of less than 5 μm away from the openings. The 1000 pA current experiment has more gallium atoms left than the 500 pA current experiment and longer FIB drilling time results more gallium contamination as expected. Therefore, it is recommended that during the fabrication, a small ion current and a short drilling time should be used to have low gallium dose and less contamination.

4. Conclusion

This work presents single cell electrophysiological measurement via sub-micrometer opening on embedded recording electrode fabricated by means of micro- and nano-machining processes. Two advantages as compared with the conventional glass-type patch clamps have been achieved. First, these devices can have electrolyte pipette resistance less than 1 MΩ with submicron opening holes to improve voltage clamp measurement and signal-to-noise ratio in experiments. Second, as a result, these devices can realize the sub-micron opening detections for possible single ion channel and small biological cell measurements. Experimentally, a 6 GΩ seal resistance for the HeLa cell and a 500 MΩ seal resistance for the yeast cell have been achieved while the electrolyte pipette resistances were 200 KΩ and 1 MΩ, respectively.

Acknowledgements

The authors would like to thank Professor Lily Jan and Ms. Helen Lai at the Department of Physiology and Biophysics in University of California at San Francisco for their help to provide HeLa cells, and Dr. Wei Liu at the Department of Chemical Engineering in University of California at Berkeley for providing yeast cells. The devices were fabricated in the Microlab at University of California at Berkeley and National Center for Electron Microscopy (NCEM) in Lawrence Berkeley National Lab.

References

[1] E. Neher, B. Sakmann, Single-channel currents recorded from membrane of denervated frog muscle-fibers, Nature 260 (5554) (1976) 799–802.
[2] A. Molleman, Patch Clamping: A Introductory Guide to Patch Clamp Electrophysiology, John Wiley & Sons Ltd., Chichester, England, 2003.
[3] A. Han, E. Moss, R.D. Rabbitt, K.L. Engisch, A.B. Frazier, A single cell multi-analysis system for electrophysiological studies, in: Proceedings of the IEEE Transducer'03, The 12th International Conference on Solid-State Sensors, Actuators and Microsystems, Boston, MA, USA, June 8–12, 2003, pp. 674–677.
[4] A. Han, E. Moss, A.B. Frazier, Whole cell electrical impedance spectroscopy for studying ion channel activity, in: Proceedings of the IEEE Transducer'05, The 13th International Conference on Solid-State Sensors, Actuators and Microsystems, Seoul, Korea, June 5–9, 2005, pp. 1704–1707.
[5] J. Seo, C. Ionescu-Zanetti, J. Diamond, R. Lal, L.P. Lee, Integrated multiple patch-clamp array chip via lateral cell trapping junctions, Appl. Phys. Lett. 84 (11) (2004) 1973–1975.
[6] C. Ionescu-Zanetti, R.M. Shaw, J. Seo, Y. Jan, L.Y. Jan, L.P. Lee, Mammalian electrophysiology on a microfluidic platform, Proc. Natl. Acad. Sci. U.S.A. 102 (26) (2005) 9112–9117.
[7] S. Pedersen, J. Kutchinsky, S. Friis, K. Krzywkowski, C.L. Tracy, R. Vestergaard, An electrophysiological lab on a chip, in: Proceedings of the IEEE Transducer'03, The 12th International Conference on Solid-State Sensors, Actuators and Microsystems, Boston, MA, USA, June 8–12, 2003, pp. 1059–1062.
[8] M. Tanabe, J. Makinodan, K. Suzuki, Y. Hosokawa, Development of micro channel array with detecting electrodes for electrophysiological biomedical sensor, in: Proceedings of the IEEE Micro Electro Mechanical Systems, Kyoto, Japan, January 19–23, 2003, pp. 407–410.
[9] R. Pantoja, J.M. Nagarah, D.M. Starace, et al., Silicon chip-based patch-clamp electrodes integrated with PDMS microfluidics, Biosens. Bioelectron. 20 (2004) 509–517.
[10] C. Schmidt, M. Mayer, H. Vogel, A chip-based biosensor for the functional analysis of single ion channels, Angew. Chem. Int. Ed. 39 (17) (2000) 3137–3140.
[11] N. Fertig, R.H. Blick, J.C. Behrends, Whole cell patch clamp recording performed on a planar glass chip, Biophys. J. 82 (2002) 3056–3062.
[12] N. Fertig, M. Klau, M. George, R.H. Blick, J.C. Behrends, Activity of single ion channel proteins detected with a planar microstructure, Appl. Phys. Lett. 81 (25) (2002) 4865–4867.
[13] N. Fertig, A. Tilke, R.H. Blick, J.P. Kotthaus, J.C. Behrends, G.T. Bruggencate, Stable integration of isolated cell membrane patches in a nanomachined aperture, Appl. Phys. Lett. 77 (8) (2000) 1218–1220.
[14] K.G. Klemic, J.F. Klemic, M.A. Reed, F.J. Sigworth, Micromolded PDMS planar electrode allows patch clamp electrical recordings from cells, Biosens. Bioelectron. 17 (2002) 597–604.
[15] K.S. Cole, J.W. Moore, Ionic current measurements in the squid giant axon membrane, J. Gen. Physiol. 44 (1960) 123–167.
[16] S. Li, L. Lin, Single cell electrophysiological analysis via sub-micrometer openings, in: Proceedings of the ASME International Mechanical Engineering Congress and Exposition, IMECE 2005-81765, Orlando, FL, November 5–11, 2005.
[17] R.A. Levis, J.L. Rae, Low-noise patch-clamp techniques, Methods Enzymol. 293 (1998) 218–266.
[18] A. Bertl, H. Bihler, C. Kettner, C.L. Slayman, Electrophysiology in the eukaryotic model cell *Saccharomyces cerevisiae*, Eur. J. Physiol. 436 (1998) 999–1013.
[19] J.G. Trapani, S.J. Korn, Control of ion channel expression for patch clamp recording using an inducible expression system in mammalian cell lines, BMC Neurosci. 4 (2003) 15–22.
[20] G.S. Hwang, K.P. Giapis, On the origin of the notching effect during etching in uniform high density plasmas, J. Vac. Sci. Technol. B 15 (1) (1997) 70–87.
[21] A. Stainshevsky, S. Aggarwal, A.S. Prakash, J. Melngailis, R. Ramesh, Focused ion-beam patterning of nanoscale ferroelectric capacitors, J. Vac. Sci. Technol. B 16 (6) (1998) 3899–3902.
[22] V. Gopal, V.R. Radmilovic, C. Daraio, S. Jin, P. Yang, E.A. Stach, Rapid prototyping of site-specific nanocontacts by electron and ion beam assisted direct-write nanolithography, Nano Lett. 4 (11) (2004) 2056–2063.

Biographies

Sha Li received her BE and ME degree from Tsinghua University, Beijing, PR China in 1999 and 2001, respectively. She is currently pursuing her PhD degree in Mechanical Engineering at the University of California at Berkeley as a Researcher at Berkeley Sensor and Actuator Center. Her research interests are in Bio-MEMS sensors, on-chip environmental control and system integration for biological applications.

Liwei Lin received his MS and PhD degrees in Mechanical Engineering from the University of California, Berkeley, in 1991 and 1993, respectively. He was with BEI Electronics Inc., Irvine, CA, from 1993 to 1994 in microsensors research and development. From 1994 to 1999, he was an Associate Professor in the Institute of Applied Mechanics, National Taiwan University, Taipei, Taiwan, and later an Assistant Professor in the Mechanical Engineering and Applied Mechanics Department at the University of Michigan, Ann Arbor. He joined the University of California, Berkeley, in 1999 and is now a Professor in the Mechanical Engineering Department and Co-Director at the Berkeley Sensor and Actuator Center, NSF/Industry/University Research Cooperative Center. His research interests are in design, modeling, and fabrication of microstructures, microsensors, and microactuators as well as mechanical issues in microelectromechanical systems. He is the holder of eight U.S. patents. Dr. Lin is the recipient of the 1998 NSF CAREER Award for research in MEMS Packaging and the 1999 ASME Journal of Heat Transfer Best Paper Award for his work on microscale bubble formation and is a Subject Editor for both the IEEE/ASME Journal of Microelectromechanical Systems and North and South American Editor of Sensors and Actuators—A Physical. He has been the founding Chairman of the ASME MEMS division since 2004 and elected ASME Fellow in 2005.